nature portfolio

https://doi.org/10.1038/s41586-025-09506-w

Supplementary information

Stabilizing effect of amino acids on protein and colloidal dispersions

In the format provided by the authors and unedited

Supporting information

Amino Acids Stabilizing Effect on Protein and Colloidal Dispersions

Ting Mao[1†], Xufeng Xu[1†], Pamina M. Winkler[1†], Cécilia Siri[1†], Ekaterina Poliukhina[1], Paulo Jacob Silva[1], Nan Xu[2], Yu Hu[2], Karim Al Zahabi[3], Rémi La Polla[1], Zhi Luo[2*], Quy Ong[1*], Alfredo-Alexander Katz[4*], Francesco Stellacci[1,5,6*]

1. Institute of Materials, Ecole Polytechnique Fédérale de Lausanne (EPFL), Lausanne, Switzerland

2. Department of Biomedical Engineering, Southern University of Science and Technology; Shenzhen 518055, Guangdong, P.R. China

3. Department of Chemical Engineering, Massachusetts Institute of Technology (MIT), Cambridge (MA), USA

4. Department of Materials Science and Engineering, Massachusetts Institute of Technology (MIT), Cambridge (MA), USA

5. Bioengineering Institute, Ecole Polytechnique Fédérale de Lausanne (EPFL), Lausanne, Switzerland

6. Global Health Institute, Ecole Polytechnique Fédérale de Lausanne (EPFL), Lausanne, Switzerland

[†]These authors contributed Equally

*Corresponding authors: luoz@sustech.edu.cn, quy.ong@epfl.ch, aalexand@MIT.EDU, francesco.stellacci@epfl.ch

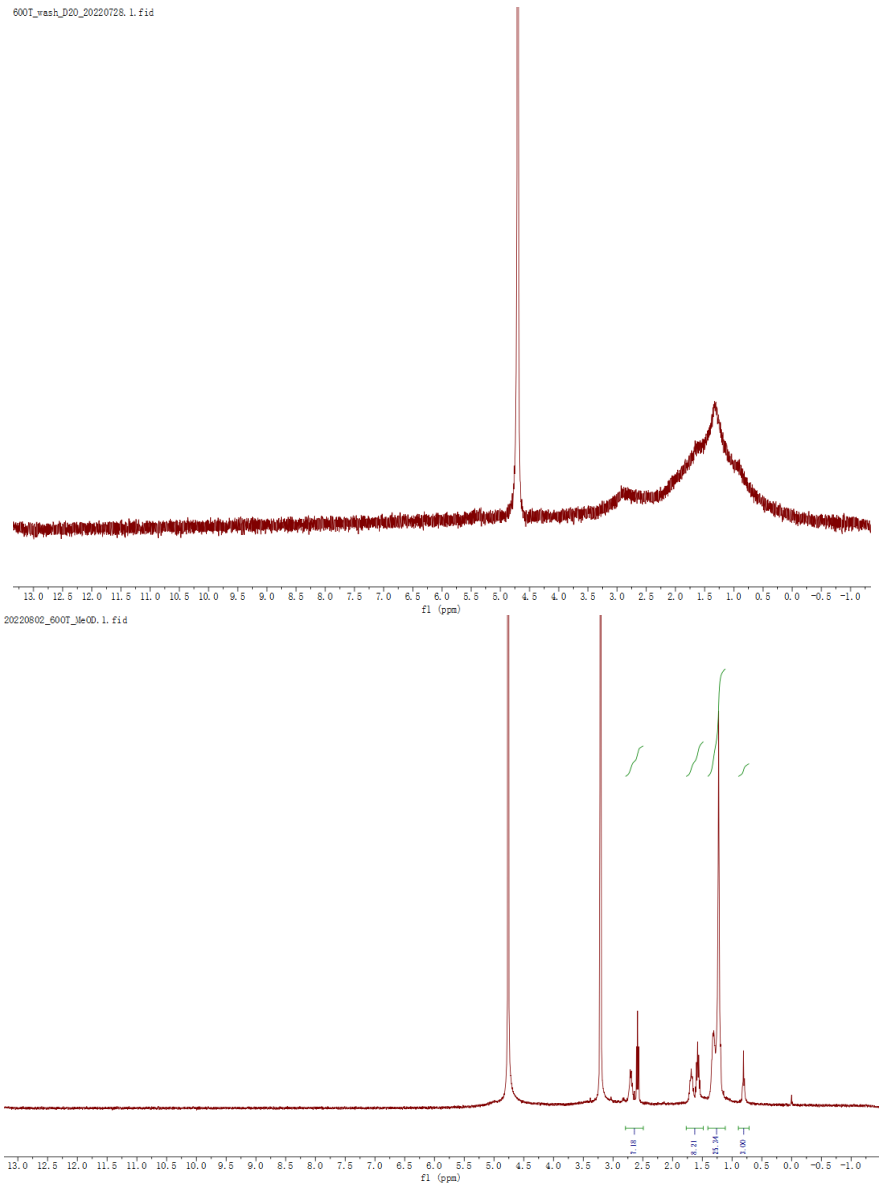

Figure S1: Top spectrum is the $1H$ NMR spectra of 56%MUS:44%OT Au nanoparticle in D_2O showing no sharp peaks of MUS indicating good quality purification of the Au nanoparticles. The bottom NMR spectra showing the same Au nanoparticle with I_2-induced ligand desorption in MeOD, with the integration of the proton signal from both the MUS and OT ligand for ligand composition calculation.

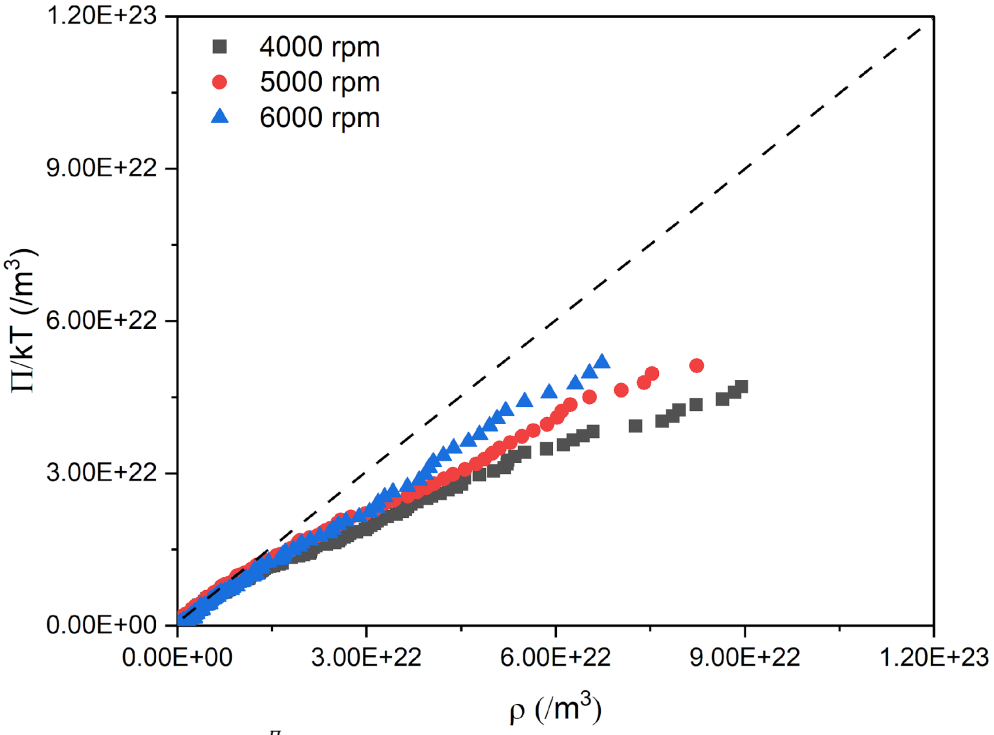

Figure S2: Osmotic pressure ($\frac{\Pi}{kT}$) versus number density (ρ) in SE-AUC experiments for MUS:OT Au NPs of 10 mg/ml in water at different angular velocities (4000, 5000, and 6000 rpm). The acceleration and deceleration were set by default 400rpm/s.

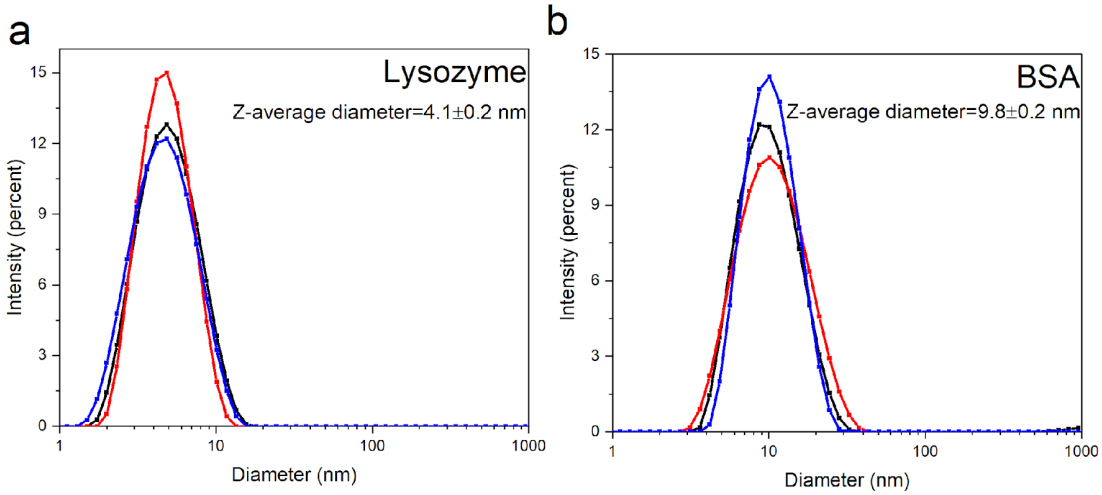

Figure S3: The hydrodynamic radius of lysozyme (a) and BSA (b) from the DLS measurements (3 replicates in black, red and blue).

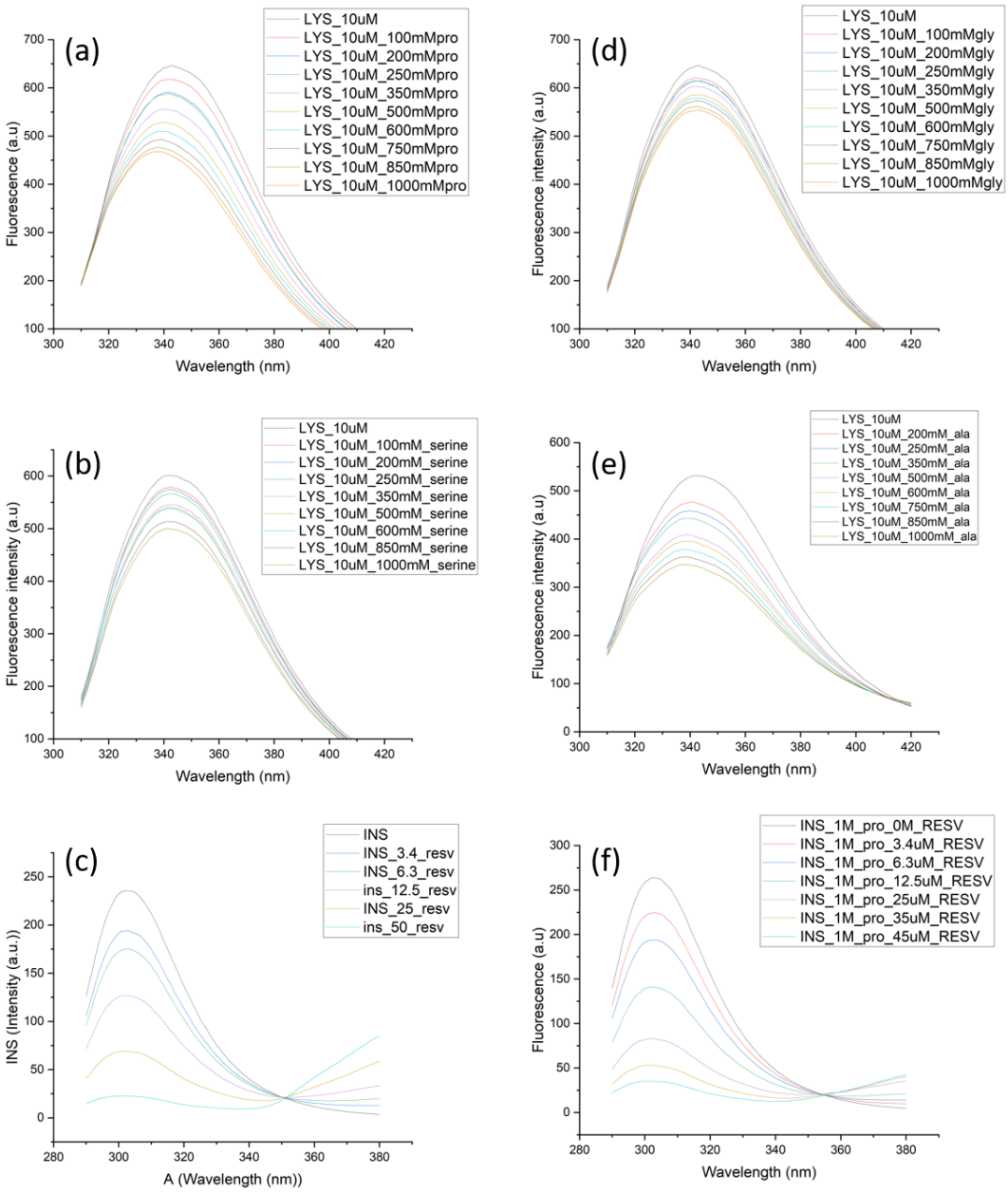

Figure S4. Data from fluorescence quenching measurements.

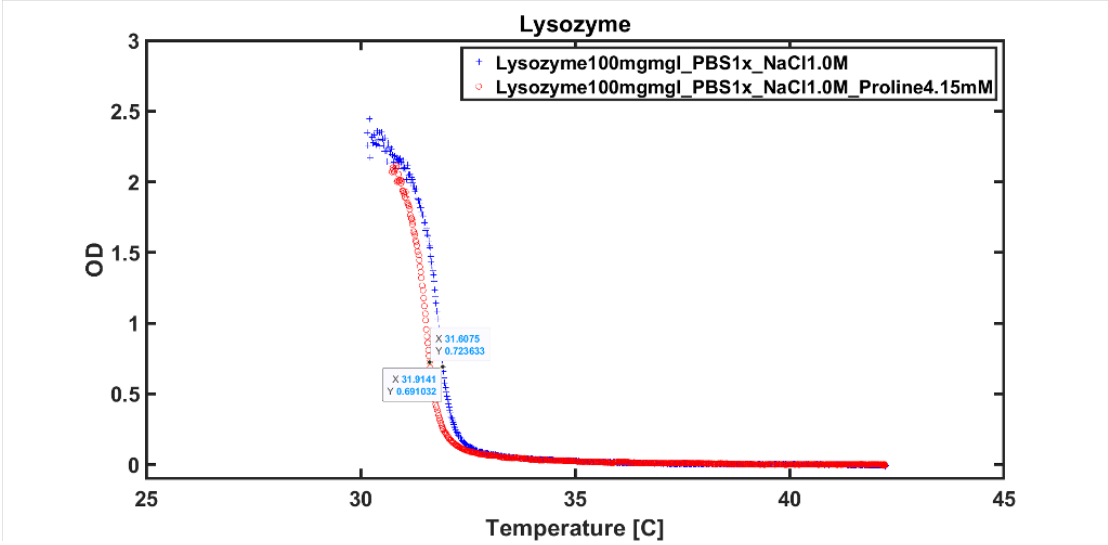

Figure S5: Cloud point measurement of the boundary temperature for the phase separation of lysozyme solution with (red)/without (blue) the presence of 4.15 mM of proline.

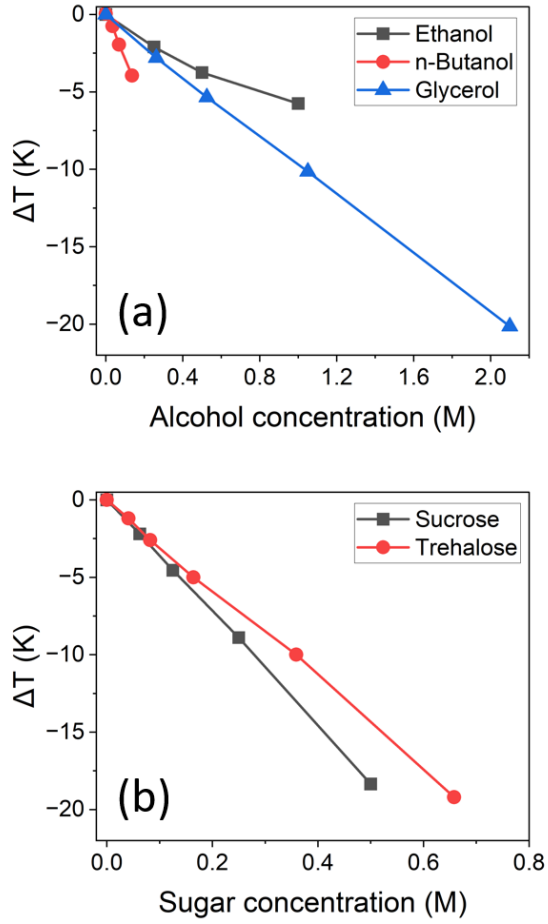

Figure S6. (a) Cloud point measurement of lysozyme in presence of ethanol, butanol, and glycerol. All the alcohols decrease the cloud point temperature. Buffer: PBS1×, 0.5M NaCl. (b). Cloud point measurement of lysozyme in presence of sugar. Both sucrose and trehalose decrease the cloud point temperature. Buffer: PBS1×, 0.5M NaCl.

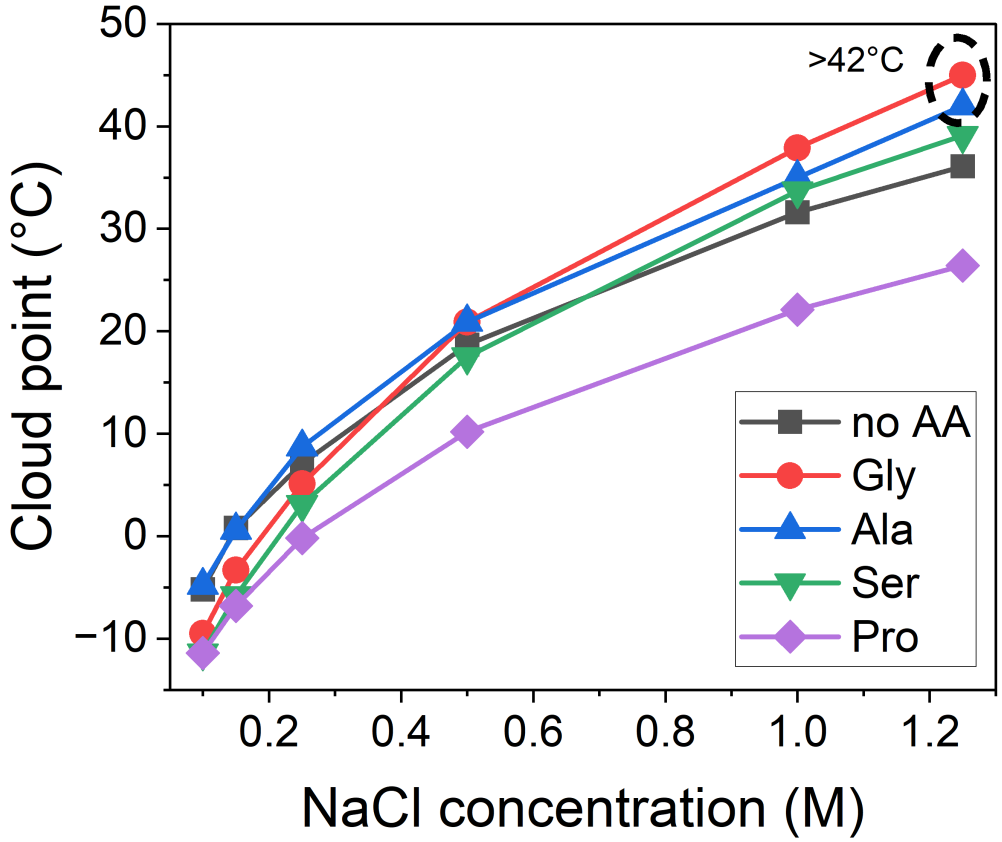

Figure S7. Cloud point measurement of lysozyme showing the competition between NaCl and amino acids (alanine, glycine). Both alanine and glycine show a threshold above which the cloud point temperature of lysozyme is higher in presence of 0.5M of amino acid than in salt alone. Included in the plot is serine which shows similar effect. Proline is included for reference. Buffer: PBS1×.

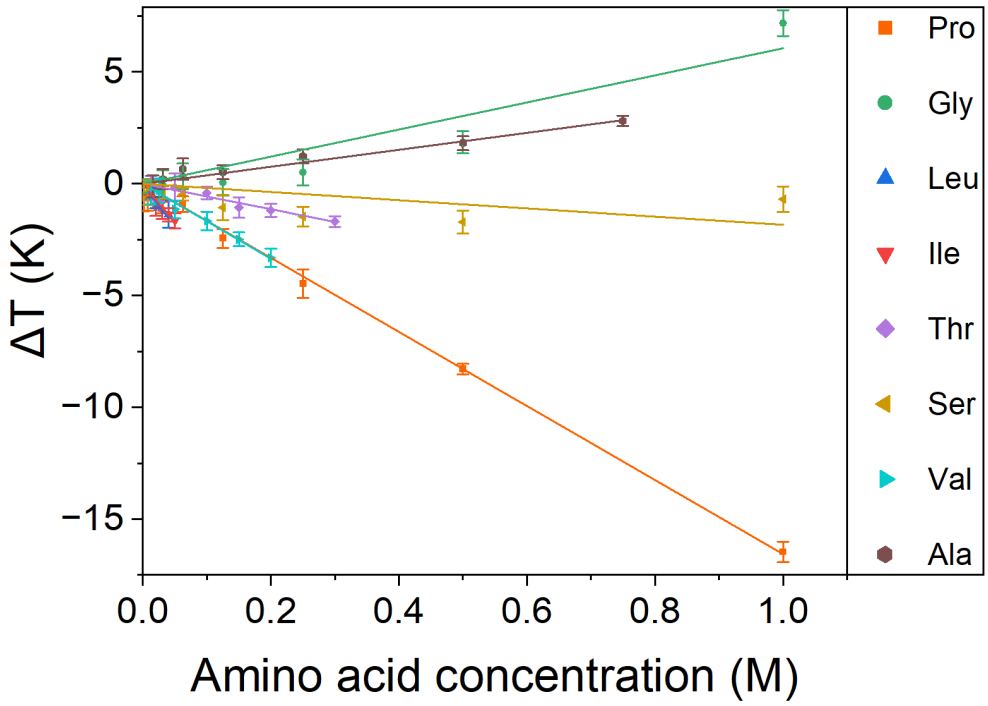

Figure S8. Cloud point measurements of lysozyme. changes of cloud point temperature of lysozyme in PBS 1× with added 0.5M NaCl with addition of different amino acids in varied concentrations.

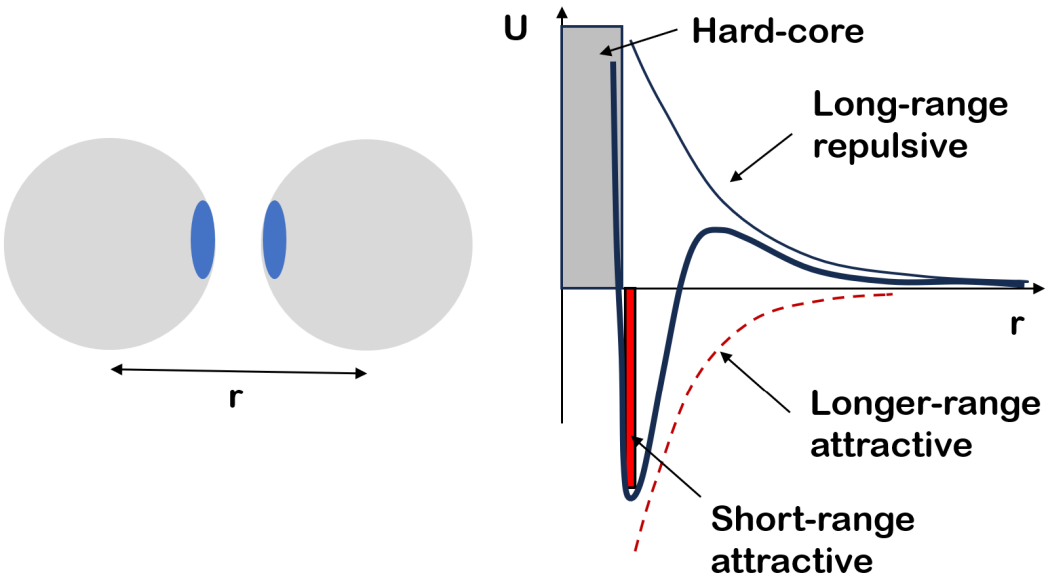

Figure S9. Patchy interaction model between two generic particles and the interaction energy consisting of different contributions and their length scale.

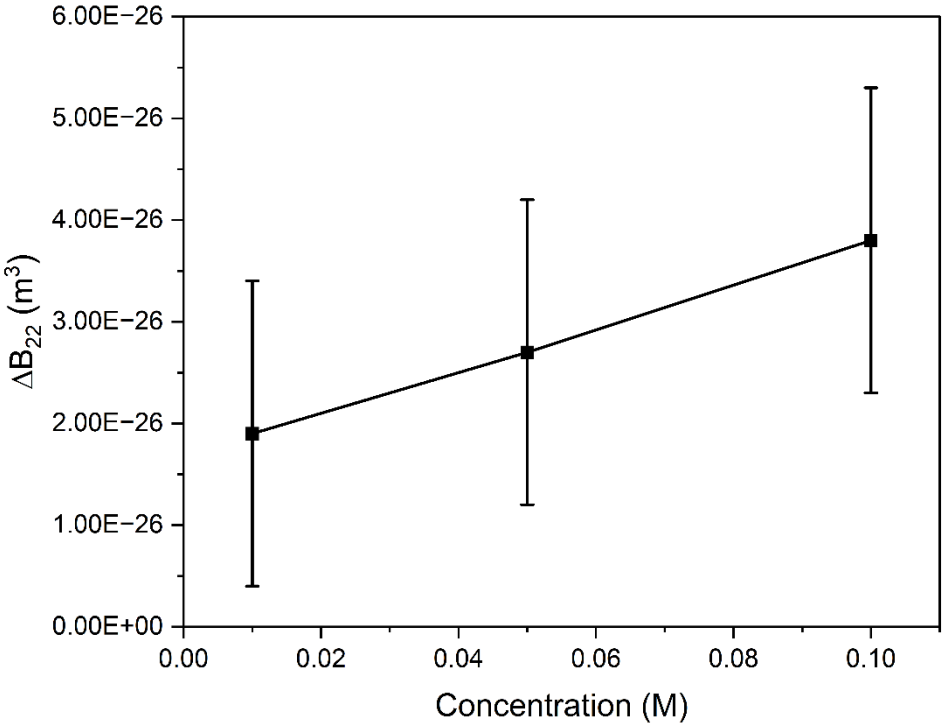

Figure S10: The change of the second virial coefficient B_{22} (ΔB_{22}) for the lysozyme-lysozyme interaction upon increasing glutamine (Gln) concentration in the low molar range by SIC.

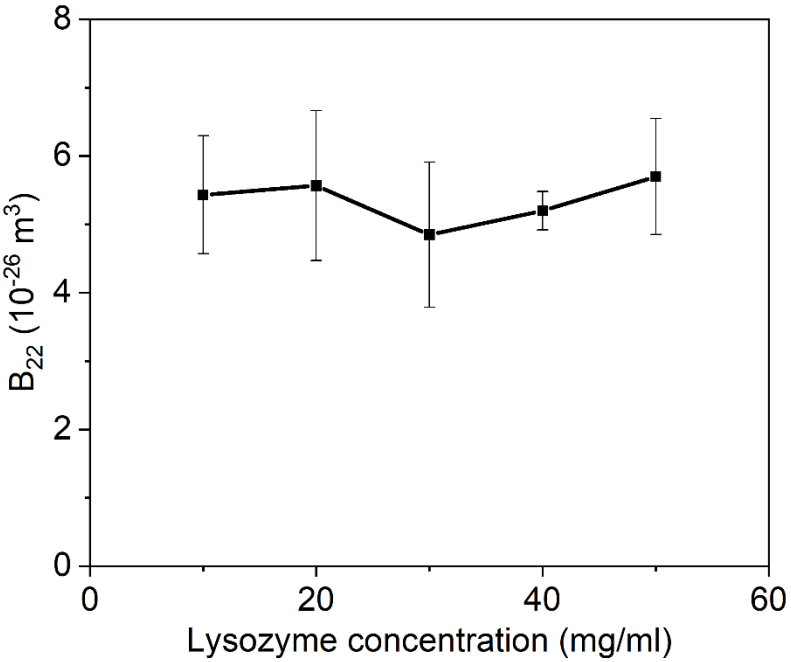

Figure S11: The second virial coefficient B_{22} for the lysozyme-lysozyme interaction at different lysozyme concentrations in presence of 0.35 M proline, obtained by applying SE-AUC experiments.

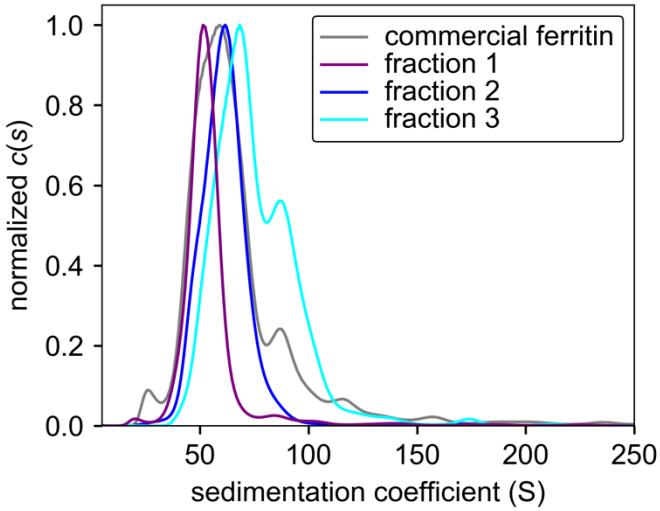

Figure S12. Sedimentation velocity c(s) profiles of the commercial ferritin before purification and the extracted three fractions after purification.

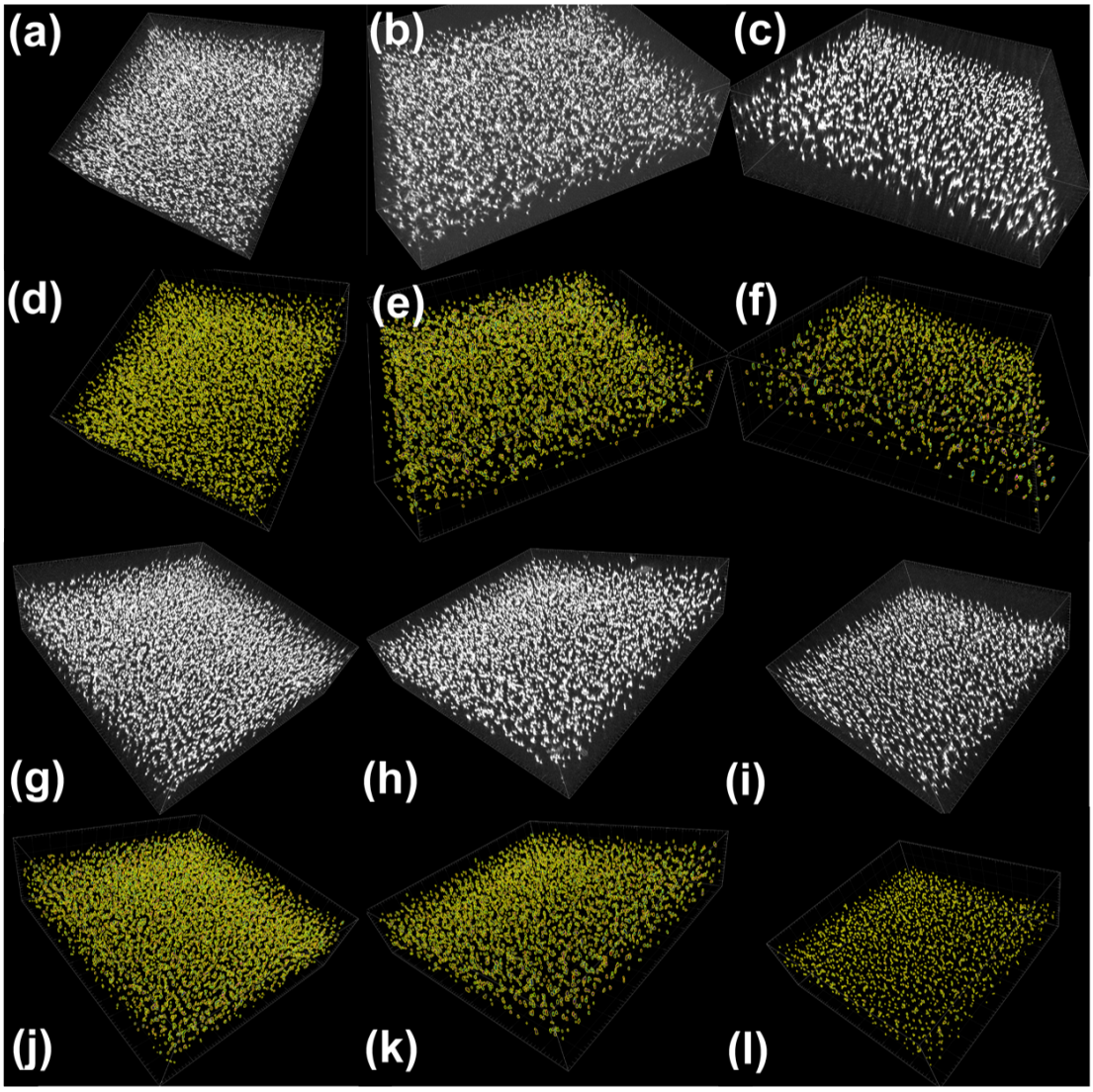

Figure S13. Examples of tomograms of sample AuNPs in water at number density in unit of $\mathrm{particles/m^3}$, 6.39×10^{22}, 5.14×10^{22}, and 3.61×10^{22} (a-c) and the identification of particles from their tomograms (d-f); Examples of tomograms of sample AuNPs in 2M proline solution at 7.01×10^{22}, 4.89×10^{22} and 3.51×10^{22} (g-i) and the identification of particles from their tomograms (j-l).

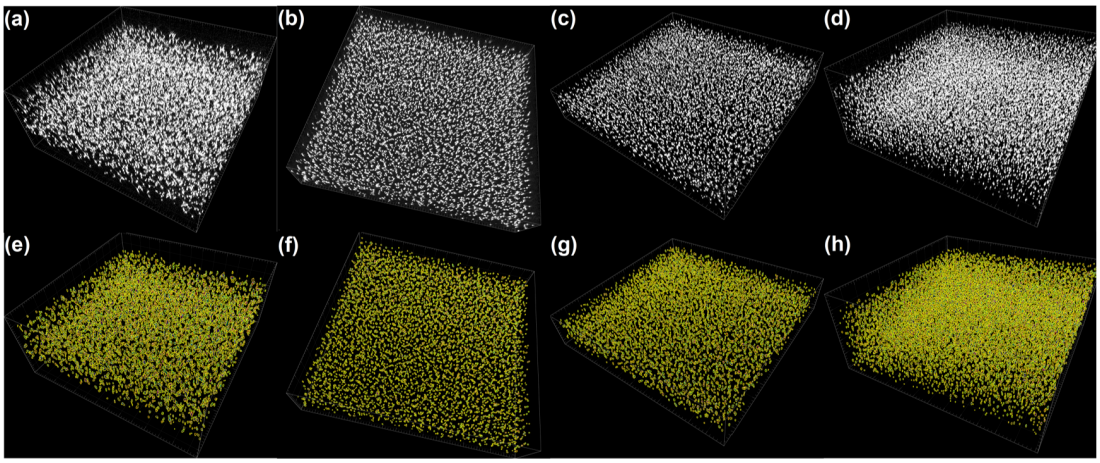

Figure S14. Examples of Au NPs tomography in water (a), 2M proline (b), 0.67 M triproline (c) and 0.5M tetraproline (d) in number density of $6.32 \times 10^{22}, 7.01 \times 10^{22}, 8.95 \times 10^{22}$ and 6.67×10^{22} $particle/m^3$ respectively and the identification of particles from their tomograms (e-h).

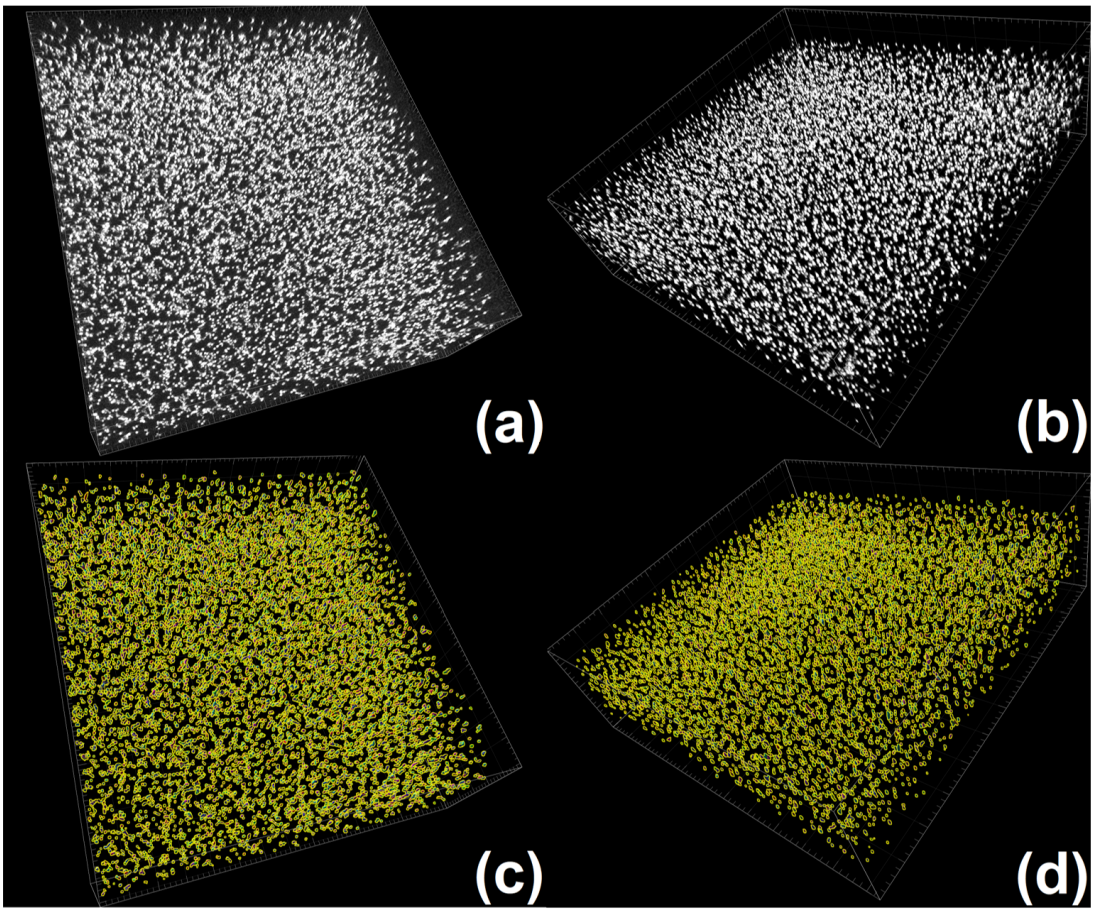

Figure S15. Examples of AuNPs in water in number density of 6.35×10^{22} $\mathrm{particle/m^3}$ (a) in contrast with the addition of 2.0 M TME in number density of 7.59×10^{22} $\mathrm{particle/m^3}$ (b) and the identification of particles from their tomograms (c, d).

	Concentration (mM)	ΔB_{22} (m^3)	SD	Technique
NaCl	500	-1.02E-25	3.00E-27	SIC
PEG 10KDa	10	-1.90E-25	7.50E-27	SIC
NaCl	500	-1.20E-25	1.34E-26	AUC
PEG 0.4KDa	100	-9.60E-27	2.30E-27	AUC

Table S1. The change of the second virial coefficient B_{22} (ΔB_{22}) for lysozyme-lysozyme interaction after the addition of 0.3 M salt (NaCl) and 0.1 M polymer (PEG 0.4 kDa) by applying SE-AUC and after the addition of 0.5 M salt (NaCl) and 0.01 M polymer (PEG 10 kDa) by applying and SIC.